Available online at www.sciencedirect.com
ScienceDirect
Journal of the European Ceramic Society 30 (2010) 187–192
www.elsevier.com/locate/jeurceramsoc

In situ photoelectron study of the (Ba,Sr)TiO_3/RuO_2 contact formation

Robert Schafranek *, Judith Schaffner, Andreas Klein

Darmstadt University of Technology, Institute of Materials Science, Petersenstrasse 23, D-64287 Darmstadt, Germany

Received 16 September 2008; received in revised form 22 April 2009; accepted 2 May 2009
Available online 31 May 2009

Abstract

The interface formation between (Ba,Sr)TiO_3 and RuO_2 has been studied using photoelectron spectroscopy. A barrier height of 0.85 ± 0.1 eV is determined. The result is discussed in relation to BST/metal interfaces, which can exhibit a variable Schottky barrier height.

Keywords: Interfaces; $BaTiO_3$ and titanates; Schottky barrier height; Fatigue; Capacitors

1. Introduction

Bariumstrontiumtitanate (BST) is widely used in electroceramic thin-film devices as ferroelectric random access memories[1] or tunable passive microwave components, e.g. phase shifters,[2] filters[3] and matching networks[4]. Device-relevant properties including leakage current,[5,6,7] insertion losses[8] or fatigue[9,10,11] are influenced by the contact properties between the ferroelectric material and the electrode. The choice of electrode material and preparation conditions have a strong influence on the Schottky barrier height for the electrons Φ_M. For BST thin films the principal mechanism for transport of charge carriers from the electrode into the ferroelectric material is thermionic emission over the Schottky barrier.[5,12] Therefore the contact properties play an important role for the optimisation of devices.

The first model proposed for the estimation of the barrier height formed at a metal/semiconductor contact was given by Schottky,[13] from which the barrier height for the electrons is derived from the difference of the work function of the metal Φ_M and the electron affinity of the semiconductor χ_S. However for the interface between Si and metals with different work functions almost no change of the Schottky barrier is observed, which was attributed to interface states pinning the Fermi level close to the middle of the band gap of Si.[14] Even for contacts where no surface states are expected, metal states can tail into the semiconductor.[15] Tersoff postulated that these metal-induced gap states (MIGS) are responsible for the barrier height formed at the metal/semiconductor interface. The MIGS have a more donor-like character close to the valence band and a more acceptor-like character near the conduction band. The energy where the interface states change their character is called branching point or charge neutrality level Φ_{CNL}.[16] The Schottky barrier height for the electrons can then be calculated from[17]:

$$\phi_{B,n} = S \cdot (\Phi_M - \Phi_{CNL}) + (\chi_S - \Phi_{CNL}) \quad (1)$$

with S beeing characteristic for a given semiconductor. $S = 1$ describes the Schottky limit, leading to the Schottky model with no pinning and $S = 0$ to the Bardeen limit of strong pinning.

RuO_2 is an interesting contact material for ferroelectric devices, as components with RuO_2 electrodes show improved fatigue and DC-degradation behaviour compared to components using Pt electrodes.[10,18] The barrier formation between RuO_2 and BST, as well as $SrTiO_3$ and $BaTiO_3$ has not been widely studied. Jeon et al. obtained a $\phi_{B,n}$ of 0.94 eV by I/V-measurements for BST deposited onto RuO_2.[19] However, the determination of barrier heights from electrical transport studies is not always unique due to the interdependence of parameters, the presence of more than one interface and only partially known transport properties of the material itself. Photoelectron spectroscopy has been widely used for many years to study semiconductor/metal interface formation.[20] This technique provides simultaneous information on electronic and chemical properties of the interfaces. It is therefore particularly suitable to identify the basic mechanisms of barrier formation and provides a direct measurement of the barrier height.

* Corresponding author. Tel.: +49 6151 166354; fax: +49 6151 166308.
E-mail address: rschafranek@surface.tu-darmstadt.de (R. Schafranek).

0955-2219/$ – see front matter © 2009 Elsevier Ltd. All rights reserved.
doi:10.1016/j.jeurceramsoc.2009.05.009

Photoelectron spectroscopic data on the interface formation of BST and RuO_2 have not been reported yet and is also scarce for further BST/electrode interfaces. Studied interfaces include (Ba,Sr)TiO_3/Pt,[21,22,23] (Ba,Sr)TiO_3/Au and (Ba,Sr)TiO_3/Cu interfaces.[24] In this work the interface formation between BST and RuO_2 is studied via photoelectron spectroscopy. The BST and RuO_2 thin film preparation and sample analysis are all carried out in the same ultra high vacuum (UHV) system (*in situ*). This allows for the characterisation of the chemical and electronical properties of contamination free surfaces and interfaces.

2. Experimental

The experiments were performed at the DArmstadt Integrated SYstem for MATerial research (DAISY-MAT), which combines a Physical Electronics PHI 5700 multitechnique surface analysis system with several deposition chambers with an UHV-sample transfer.[25] X-Ray photoelectron (XP) spectra were recorded using monochromatic Al K_α radiation with an energy resolution of ≈0.4 eV as determined from the broadening of the Fermi edge of a sputter cleaned Ag sample. Ultraviolet photoelectron (UP) spectra were measured in normal emission with HeI excitation and a sample bias of −1.5 V. The preparation of the 200 nm thin BST film was performed by RF magnetron sputtering from a 2 in. diameter ceramic $Ba_{0.6}Sr_{0.4}TiO_3$-target, using a sputter power density of 2 W/cm^2, a substrate to target distance of 5 cm, a pressure of 5 Pa, an Ar/O_2-ratio of 99/1 and a substrate temperature of 650 °C. Commercially available Si(0.3 mm)(1 0 0)/SiO_2(300 nm)/TiO_2(20 nm)/Pt(150 nm)(1 1 1) substrates from Inostek were used. Similarly prepared BST thin films showed a capacitance tunability of 28.1% at an applied field of 500 kV/cm and a maximal loss tangent of 0.0032.[8]

The RuO_2 thin films used for the interface characterisation are deposited by reactive DC magnetron sputtering from a 2 inch diameter metallic Ru target, using a power density of 2 W/cm^2, a substrate to target distance of 10 cm, a pressure of 1 Pa, an Ar/O_2-ratio of 85/15 and no substrate heating. The deposition rates for BST and RuO_2 are 7 nm/min and 20 nm/min, respectively. No contaminations and no other emissions than Ba, Sr, Ti and O for BST and Ru and O for RuO_2 can be observed, as verified in Fig. 1.

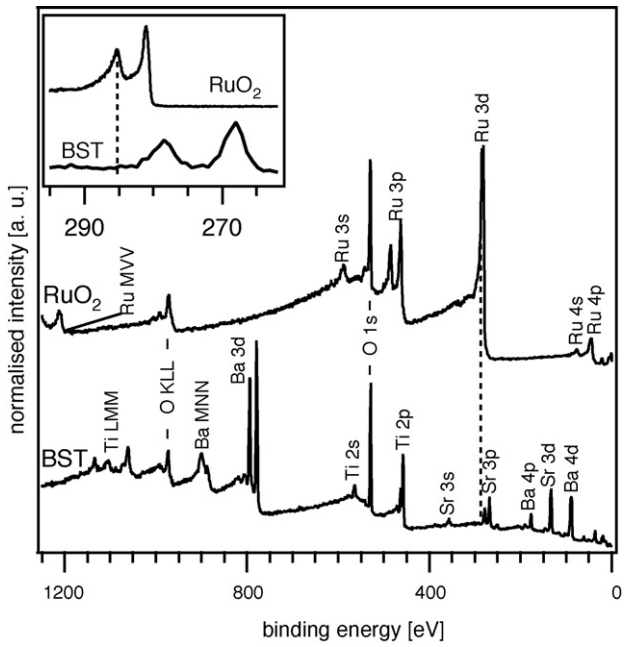

Fig. 1. XP-Survey spectra of the 200 nm thick BST thin film and the 5 nm thick RuO_2-thin film deposited on BST. Only emissions corresponding to the respective thin films are observed. No carbon contaminations are present on the BST sample, as can be deduced from the absence of a feature at 285 eV (as indicated by the dotted line), where the C 1s emission is expected. For RuO_2 a detail spectrum of the Ru 3d emission is shown in the insert. The spectra can be fully described by the Ru 3d dublett without an C 1s emission at ≈285 eV, as expected for carbon contaminations.

3. Results

3.1. Surface properties of RuO_2 and BST

In Fig. 2(a) the XP-spectra of the Ru $3d_{5/2}$ and O 1s core level emissions as well as of the X-ray excited valence bands are shown for the reactively sputtered RuO_x-thin films in dependence on oxygen content in the Ar/O_2 sputter gas mixture. The thin film sputtered with pure Ar still shows a small O emission, which is attributed to the base pressure of the deposition chamber of 10^{-5} Pa, beeing not low enough to prepare oxygen free Ru thin film surfaces. With increasing oxygen content of 5 and 7.5% in the sputter gas, the Ru^0 as well as Ru^{4+} emission are observed in the Ru spectra, as indicated. The valence band spectra recorded with XPS (Fig. 2(a)) and UPS (Fig. 2(b)) for the films prepared with less then 10% O_2 do not show the characteristic shape observed for RuO_2.[26] Therefore films deposited with 5 and 7.5% O_2 in the sputter gas are composed of substoichiometric RuO_{2-x}. In contrast, films deposited with an O_2 content ≥ 10% show only the Ru^{4+} emission and a valence band form characteristic for RuO_2. RuO_2 shows metallic conduction because of a partly filled 4d band.[27] The Ru 4d derived band exhibits a maximum 0.7 eV below the Fermi energy, [27] explaining the characteristic form of the RuO_2 valence band spectra below E_F. The barely visible features at 4 and 7 eV are derived from the interaction of the Ru 4d and O 2p bands.[26]

The work function Φ of the deposited thin films is deduced from the secondary electron onset presented in Fig. 2(b). The Ru thin film prepared without oxygen in the sputter gas exhibits $\Phi = 5.3$ eV. This value is considerably larger than the work function of 4.71 eV reported for polycrystalline Ru.[28] The difference in work function can be attributed to the different preparation conditions of the Ru thin film. Nieuwenhuys et al. reported a maximum pressure of 5×10^{-8} Pa during Ru thin film preparation via Ru evaporation, leading to pure Ru surfaces. For the sputtered Ru film O is present on the surface, as mentioned before.

The work function increases with increasing O_2 content in the sputter gas. For the RuO_2 thin films sputtered with 10 and 12.5% O_2 a work function of 6.1 ± 0.05 eV is found. Experimental values for the work function of RuO_2 (as measured by UPS) are very limited. Hartman et al. have studied the work

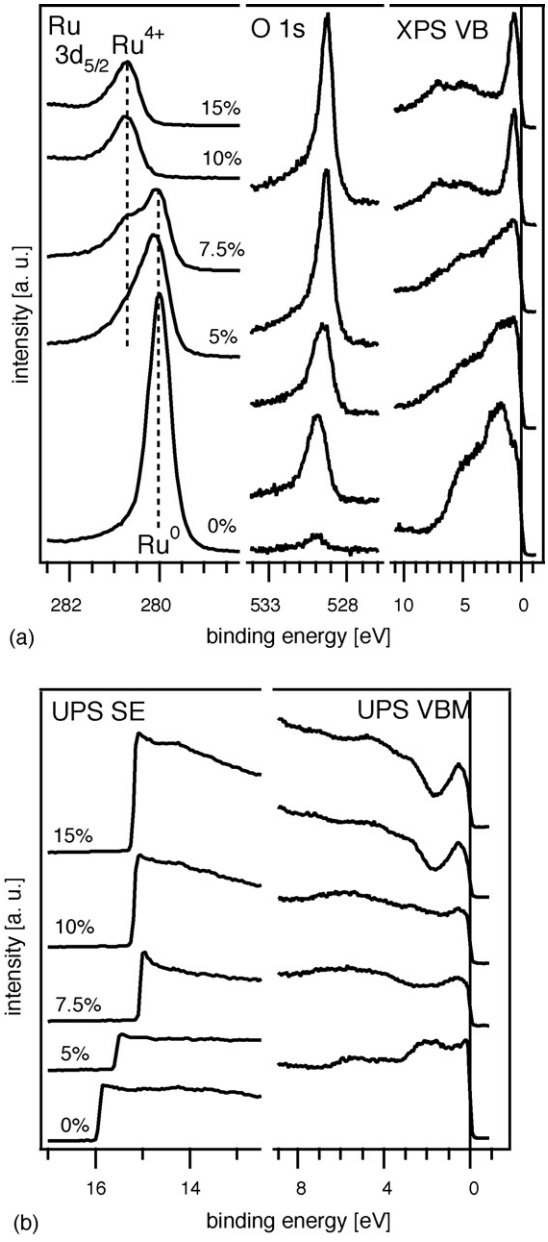

Fig. 2. (a) XP-spectra of the Ru $3d_{5/2}$, O 1s and valence band and (b) UP-spectra of the secondary electron onset and the valence band are shown for different O_2-contents in the Ar/O_2 gas mixture during sputter deposition. With an O_2-content $\geq$ 10% RuO_2 is formed, as deduced from Ru and valence band spectra.

function of RuO_x by oxidizing metal Ru films at 400 °C, 500 °C and 600 °C in air. The samples showed a surface carbon contamination and a work function of 4.6 eV for the unoxidized sample as well as for the samples annealed at 400 °C and 500 °C in air. These samples showed compositions of RuO_x with $x < 2$. For the sample heated at 600 °C, where no more Ru^0 emission was observed, the authors found a work function of 5.0 eV.

This is in strong contrast to our observations and could be explained by the adsorbed contaminations on the RuO_x thin films studied by Hartman et al. Since the authors did not present survey and UP-Spectra of the RuO_x films, further discussion of the discrepancy in the work function determination is not possible.

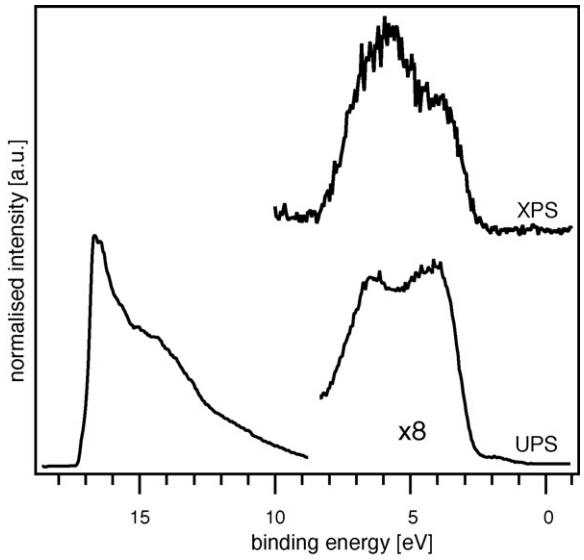

Fig. 3. UP-spectrum and XP-spectrum of the 200 nm thick BST thin film. A work function of 4.4 eV is found for BST. The intensity of the UP valence band below 8 eV is multiplied by 8 for better visibility. The distance of the valence band maximum to the Fermi energy for BST is 2.45 eV, as deduced from XPS.

In Fig. 3 the XP and UP valence band spectra and the secondary electron onset of the BST thin film are presented. The spectra are normalized to the same intensity. The valence band of the BST thin film exhibits the well known emission features at 6.5 and 4 eV, which are attributed to bonding O 2p states mixed with Ti 3d states for the first, and non-bonding O 2p states for the latter.[29,30] The valence band maximum (VBM) position, as deduced from the intercept of the leading edge of the valence band with the background lies at 2.45 eV, as measured with XPS and at 2.65 eV, as measured with UPS. The 0.2 eV higher binding energy position of the valence band maximum, as deduces from UPS, could be related to the energy-dependence of the photoionisation cross-sections and different surface sensitivities of UPS and XPS.[30] Sample charging could also account for a higher VBM position measured with UPS. However, since the samples show a low VBM binding energy position compared to literature values,[31,32] charging is ruled out. The variation of the photoionisation cross-sections with energy is also responsible for the different ratios of the features at 6.5 and 4 eV as measured with UPS and XPS. The work function can be deduced from the secondary electron onset and lies at 4.4 ± 0.05 eV. This leads to an ionization potential of 7.0 ± 0.1 eV and an electron affinity of 3.9 ± 0.1 eV, taking the band gap of BST of 3.2 eV[33] into account.

3.2. Interface formation

In Fig. 4 the spectra of the Ba $3d_{5/2}$, Sr 3d, Ti 2p, O 1s and Ru 3d emission lines are shown for the bare BST thin film substrate and after stepwise deposition of RuO_2. The attenuation of the substrate emissions of Ba, Sr and Ti as well as the growth of the Ru emission can be observed with increasing RuO_2 thickness. The form of the O emission changes gradually with increasing thickness of RuO_2 from the symmetric lineform

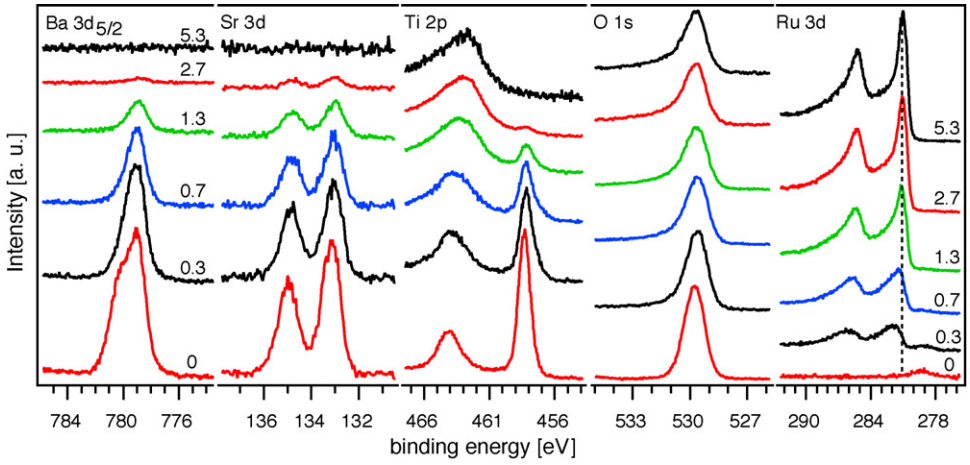

Fig. 4. XP-Spectra of the Ba $3d_{5/2}$, Sr 3d, Ti 2p, O 1s and Ru 3d emission lines with increasing RuO_2 thickness given in nm. No obvious interface reaction and a parallel shift of the substrate emission lines can be observed.

observed for insulators, to a shape with an asymmetry to higher binding energies. The same holds true for the Ru emission and is explained by the metallic character of RuO_2, which gives rise to an asymmetric Doniach–Sunjic line profile.[34] While the shape of the Sr emission shows no observable change during the RuO_2-deposition, the form of the Ti emission is altered. This is obviously due to the underlying Ru $3p_{1/2}$-emission, which is also present after thick RuO_2 deposition. Nonetheless the binding energy position of the Ti emission can be reliably extracted.

In Fig. 5(a) the evolution of the Fermi energy position in the band gap of BST is presented with increasing RuO_2-thickness. For monitoring the distance of the valence band maximum to the Fermi energy $E_F - E_{VBM}$ during the interface experiment, only core level binding energies of Sr and Ti can be used, as the valence band and the oxygen emission of BST and RuO_2 superimpose during the interface experiment. As we do not observe an interface reaction and the Sr and Ti emissions show a parallel shift, we can reliably assume a parallel shift of the BST valence band maximum with the BST core level lines. Starting from $E_F - E_{VBM} = 2.45$ eV, as determined from XPS valence band of the uncovered BST substrate, $E_F - E_{VBM}$ shifts towards 2.35 eV when the RuO_2 exceeds unit cell thickness. Using the band gap of 3.2 eV for BST,[33] this amounts to a Schottky barrier height for the electrons of 0.85 eV with a typical uncertainty of the barrier height determination of 0.1 eV. This value is in good agreement with I–V measurements, where a $\phi_{B,n}$ of 0.94 eV was found for BST deposited onto RuO_2.[19] The resulting band diagram for the BST/RuO_2 contact is given in Fig. 5(b).

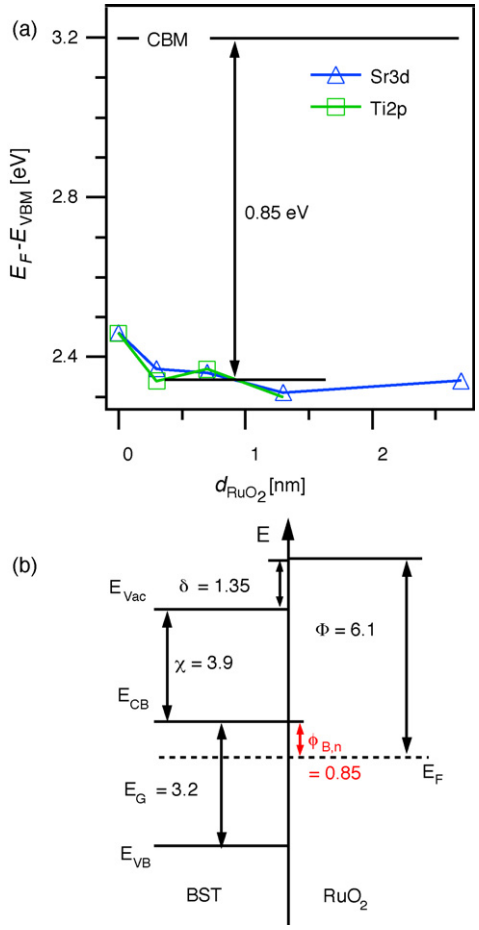

Fig. 5. (a) Presentation of the distance of the valence band maximum to the Fermi energy $E_F - E_{VBM}$ as determined from the substrate emission lines Sr and Ti with increasing RuO_2 thickness d_{RuO_2}. A Schottky barrier height of 0.85 eV can be deduced, taking the band gap of BST of 3.2 eV into account. (b) Schematic band diagram for the BST/ RuO_2-contact. Although RuO_2 and BST show a large difference in work function and electron affinity χ, a relatively small $\phi_{B,n}$ of 0.85 eV is formed due to the high surface dipole $\delta = 1.35$ eV. Energies in the schematic are given in eV.

4. Discussion

Using the simple Schottky model, as done by Scott[35] for the BST/electrode-interface, a barrier height for the electrons of 2.2 eV is estimated from the difference in work function of 6.1 eV for RuO_2 and the electron affinity of 3.9 eV for BST. In the Schottky model metal-induced gap states or interface defect states are not taken into account. Robertson et al. have calculated Schottky barriers heights for electrons for different metals with $SrTiO_3$.[17] The authors used a charge neutrality level

0.7 eV below the conduction band minimum, as deduced with the Cardona–Christensen method[36] and a value for S of 0.28, as calculated after the empirical formula derived by Moench for $\epsilon_\infty = 6.1$[16]:

$$S = \frac{1}{1 + 0.1(\epsilon_\infty - 1)^2} \quad (2)$$

Robertson et al. calculated barrier heights of 0.84 and 0.89 eV for $SrTiO_3$/Au and $SrTiO_3$/Pt interfaces using work functions of 5.1 and 5.3 eV, respectively. With the same values for Φ_{CNL} and S a Schottky barrier height for the electrons of 1.12 eV can be calculated using the work function of 6.1 eV found for RuO_2. The experimentally determined value for the barrier height at the BST/RuO_2 contact of 0.85 ± 0.1 eV is in close agreement to the calculated barrier height and supports a strong Fermi level pinning at the (Ba,Sr)TiO_3/RuO_2 contact. The difference between the calculated and experimentally determined barrier height might be explained by a slightly shallower position of the charge neutrality level or a smaller value of S compared to the values used by Robertson et al.

The technically important BST/Pt interface has been thoroughly studied using electrical measurements. A variation of the Schottky barrier height of 0.5–1.6 eV was found[37,38] and the difference of the $\phi_{B,n}$ could be attributed to preparation and subsequent annealing conditions. While after deposition relatively small $\phi_{B,n} \approx 0.6$ eV are found, an annealing step in an oxygen containing atmosphere leads to an increase in $\phi_{B,n}$ to ≈ 1.2 eV[39,7]. *In situ* photoelectron studies of the contact formation between strontium titanate (STO) and Pt directly after Pt deposition lead to $\Phi_{B,n}$ of 0.4–0.6.[21,22,23] The barrier height increases to $\phi_{B,n} \geq 1.2$ eV after heating in an oxygen atmosphere.[23] The microscopic origin for the variation of $\phi_{B,n}$ has been identified as formation of defects at the STO/Pt interface upon Pt deposition due to the high Pt condensation enthalpy. These defects pin the Fermi level close to the conduction band minimum and therefore lead to a small $\phi_{B,n}$. Upon annealing in oxygen the concentration of these defects is reduced and a high $\phi_{B,n}$ is formed.[23] Similar Observation have been made for the SnO_2/Pt interface.[40] Oxidation and reduction of the interface is not likely for RuO_2 electrodes. This is also supported by comparing the results of this work for RuO_2 deposited onto BST to BST deposition onto RuO_2 as done by Jeon et al.[19] The same barrier height is observed for both deposition sequences, in contrast to strongly different barrier heights at the as-deposited BST/Pt and Pt/BST interface.[23]

Although RuO_2 exhibits a work function $\Phi = 6.1$ eV, which is 0.4 eV larger than that of Pt ($\Phi = 5.7$ eV),[23] the Schottky barrier height is considerably smaller at the BST/RuO_2 interface than at the oxidized BST/Pt interface.

The usually observed larger leakage current for metal/ferroelectric/metal structures using RuO_2 as electrode compared to Pt[10,9] is well explained by the larger Schottky barrier at oxidized BST/Pt interfaces.

Oxidic electrodes as RuO_2 are nonetheless highly interesting, especially when the fatigue or DC-degradation behaviour of the studied device is of interest, since they show smaller or no observable degradation over the studied timeframe or cycles.[10,18,11] One possible explanation for the better performance with oxidic electrodes regarding fatigue might be the fact that the BST/Pt-interface, as well as other BST/metal interfaces show two different states for the Schottky barrier height. On the one hand a reduced interface with a small $\phi_{B,n}$ and on the other hand an oxidized interface with a high $\phi_{B,n}$. For Pt/PZT/Pt-capacitors an annealing step in oxygen after Pt top electrode deposition leads to a considerable increase of the remanent polarization.[41] This rise in polarisation is in parallel with an increase in $\phi_{B,n}$ as was discussed before. Angadi et al. have found an increase of the dielectric loss in parallel with the onset of the fatigue of studied Pt/PZT/Pt-capacitors. Higher dielectric loss can be attributed to a reduction of the Schottky barrier height.[8]

This suggests that a reduction of the Schottky barrier height during voltage-stressing, as induced, e.g. by electric-field driven migration of oxygen vacancies to the electrode, might be related to the degradation with metallic electrodes. In contrast, the oxidic electrodes do not show this effect and therefore exhibit an improved device stability.

5. Conclusions

RuO_2 was deposited via reactive DC-magnetron sputtering on thin film BST. The deposition conditions for RuO_2 have been appropriately chosen as to be in the compound regime for reactive sputtering, not to deposit substoichiometric RuO_{2-x}. Work functions of 6.1 eV for RuO_2 and of 4.4 eV for BST and an electron affinity of 3.9 eV for the latter were observed. The interface formation was analysed via *in situ* photoelectron spectroscopy. No interface reaction and a parallel shift of the substrate levels were observed. A Schottky barrier height for the electrons of 0.85 ± 0.1 was deduced for the BST/RuO_2-interface. This is in accordance with I/V-measurements of the RuO_2/BST interface found in the literature. [19] The barrier height is smaller than expected from the Schottky model (2.2 eV) and is in close agreement with the charge neutrality model (1.12 eV). Compared to the BST/Pt interface, where a high and low Schottky barrier height are possible,[23] the BST/RuO_2 interface probably exhibits a unique barrier height as suggested by comparing the BST/RuO_2 and RuO_2/BST-interfaces. These findings might be related to the reduced fatigue of devices having oxidic electrodes as RuO_2 in contrast to devices featuring metallic electrodes.

Acknowledgements

This work was supported by the German Research Foundation (DFG) within the DFG Research Training Group 1037 "Tunable integrated components in microwave technology and optics (TICMO)" and within the DFG Collaborative Research Centre 595 "Electrical Fatigue in Functional Materials".

References

[1]. Scott, J.F., Ferroelectric Memories, Springer, New York, 2000.
[2]. Kozyrev, A., Ivanov, A., Keis, V., Khazov, M., Osadchy, V., Samoilova, T., Soldatenkov, O., Pavlov, A. and Koepf, G., Ferroelectric films: nonlinear

properties and applications in microwave devices. In *Microwave Symposium Digest, 1998*, 1998, pp. 985–988.
[3]. Tombak, A., Maria, J. P., Ayguavives, F. T., Jin, Z., Stauf, G. T., Kingon, A. I. and Mortazawi, A., Voltage-controlled rf filters employing thin-film barium–strontium–titanate tunable capacitors. *IEEE Transactions on Microwave Theory and Techniques*, 2003, **51**(2), 462–467.
[4]. Scheele, P., Goelden, F., Giere, A., Mueller, S. and Jakoby, R., Continuously tunable impedance matching network using ferroelectric varactors. In *Microwave Symposium Digest, 2005*, 2005, pp. 6500–6512.
[5]. Abe, K. and Komatsu, S., Epitaxial-growth of $SrTiO_3$ films on Pt electrodes and their electrical-properties. *Japanese Journal of Applied Physics Part 1—Regular Papers Short Notes and Review Papers*, 1992, **31**(9B), 2985–2988.
[6]. Fukuda, Y., Nagoshi, M., Suzuki, T., Namba, Y., Syono, Y. and Tachiki, M., Chemical states of Ba in $YBa_2Cu_3O_{7-\delta}$ studied by x-ray photoelectron spectroscopy. *Physical Review B*, 1989, **39**(16), 11494.
[7]. Cramer, N., Mahmud, A. and Kalkur, T. S., Effect of annealing on leakage current in $Ba_{0.5}Sr_{0.5}TiO_3$ and $Ba_{0.96}Ca_{0.04}Ti_{0.84}Zr_{0.16}O3$ thin films with Pt electrodes. *Applied Physics Letters*, 2005, **87**(3), 32903.
[8]. Schafranek, R., Giere, A., Balogh, A. G., Enz, T., Zheng, Y., Scheele, P., Jakoby, R. and Klein, A., Influence of sputter deposition parameters on the properties of tunable barium strontium titanate thin films for microwave applications. *Journal of the European Ceramic Society*, 2009, **29**, 1433–1442.
[9]. Alshareef, H. N., Kingon, A. I., Chen, X., Bellur, K. R. and Auciello, O., Contribution of electrodes and microstructures to the electrical-properties of $Pb(Zr_{0.53}Ti_{0.47})O_3$ thin-film capacitors. *Journal of Materials Research*, 1994, **9**(11), 2968–2975.
[10]. Lichtenwalner, D., Dat, R., Auciello, O. and Kingon, A. I., Effect of electrodes on the ferroelectric properties of pulsed-laser ablation-deposited $PbZr_xTi_{1-x}O_3$ thin film capacitors. *Ferroelectrics*, 1994, **152**, 97–102.
[11]. Masuda, Y. and Nozaka, T., The influence of various upper electrodes on fatigue properties of perovskite $Pb(Zr,Ti)O_3$ thin films. *Japanese Journal of Applied Physics Part 1—Regular Papers Short Notes and Review Papers*, 2003, **42**(9B), 5941–5946.
[12]. Dietz, G. W., Antpohler, W., Klee, M. and Waser, R., Electrode influence on the charge-transport through $SrTiO_3$ thin-films. *Journal of Applied Physics*, 1995, **78**(10), 6113–6121.
[13]. Schottky, W., *Zeitschrift fuer Physik*, 1940, **41**, 570.
[14]. Bardeen, J., Surface states and rectification at a metal semiconductor contact. *Physical Review*, 1947, **71**(10), 717–727.
[15]. Heine, V., Theory of surface states. *Physical Review*, 1965, **138**(6), 1689–1696.
[16]. Moench, W., Role of virtual gap states and defects in metal-semiconductor contacts. *Physical Review Letters*, 1987, **58**(12), 1260.
[17]. Robertson, J. and Chen, C. W., Schottky barrier heights of tantalum oxide, barium strontium titanate, lead titanate, and strontium bismuth tantalate. *Applied Physics Letters*, 1999, **74**(8), 1168–1170.
[18]. Angadi, M., Auciello, O., Krauss, A. R. and Gundel, H. W., The role of electrode material and polarization fatigue on electron emission from ferroelectric $Pb(Zr_xTi_{1-x})O_3$ cathodes. *Applied Physics Letters*, 2000, **77**(17), 2659–2661.
[19]. Jeon, M. S. and Choi, D. K., Influences of the $(Ba,Sr)TiO_3$-modified RuO_2 interface on the dielectric constant and current–voltage characteristics. *Journal of Vacuum Science and Technology B*, 1997, **15**(4), 928–934.
[20]. See, e.g., the Conference Records of the International Conference on Physics and Chemistry of Semiconductor Interfaces (PCSI), unpublished.
[21]. Chung, Y. W. and Weissbard, W. B., Surface spectroscopy studies of the $SrTiO_3$ (1 0 0) surface and the Platinum–$SrTiO_3$ (1 0 0) interface. *Physical Review B*, 1979, **20**(8), 3456–3461.
[22]. Copel, M., Duncombe, P. R., Neumayer, D. A., Shaw, T. M. and Tromp, R. M., Metallization induced band bending of $SrTiO_3$ (1 0 0) and $Ba_{0.7}Sr_{0.3}TiO_3$. *Applied Physics Letters*, 1997, **70**(24), 3227–3229.
[23]. Schafranek, R., Payan, S., Maglione, M. and Klein, A., Barrier height at $(Ba,Sr)TiO_3$/Pt interfaces studied by photoemission. *Physical Review B*, 2008, **77**, 195310.
[24]. Schafranek, R. and Klein, A., In situ photoemission study of the contact formation of $(Ba,Sr)TiO_3$ with Cu and Au. *Solid State Ionics*, 2006, **177**, 1659.
[25]. Ensling, D., Thißen, A., Gassenbauer, Y., Klein, A. and Jaegermann, W., In-situ preparation and analysis of functional oxides. *Advanced Engineering Materials*, 2005, **7**, 945–949.
[26]. Riga, J., Tenret, N., l, C., Pireaux, J. J., Caudano, R., Verbist, J. J. and Gobillon, Y., Electronic structure of rutile oxides TiO_2, RuO_2 and IrO_2 studied by X-ray photoelectron spectroscopy. *Physica Scripta*, 1977, **16**(5–6), 351–354.
[27]. Glassford, K. M. and Chelikowsky, J. R., Electronic and structural properties of RuO_2. *Physical Review B*, 1993, **47**(4), 1732.
[28]. Nieuwenhuys, B. E., Bouwman, R. and Sachtler, W. M. H., The changes in work function of group ib and viii metals on xenon adsorption, determined by field electron and photoelectron emission. *Thin Solid Films*, 1974, **21**(1), 51–58.
[29]. Henrich, V. E., Dresselhaus, G. and Zeiger, H. J., Surface defects and the electronic structure of $SrTiO_3$ surfaces. *Physical Review B*, 1978, **17**(12), 4908.
[30]. Henrich, V. and Cox, P., *The Surface Science of Metal Oxides*. Cambridge University Press, Cambridge, 1994.
[31]. Amy, F., Wan, A., Kahn, A., Walker, F. J. and McKee, R. A., Surface and interface chemical composition of thin epitaxial $SrTiO_3$ and $BaTiO_3$ films: photoemission investigation. *Journal of Applied Physics*, 2004, **96**(3), 1601–1606.
[32]. Quan, Z., Zhang, B. S., Zhang, T. J., Zhao, X. Z., Pan, R. K., Ma, Z. J. and Jiang, J., Interfacial characteristics and dielectric properties of $Ba_{0.65}Sr_{0.35}TiO_3$ thin films. *Thin Solid Films*, 2008, **516**(6), 999–1005.
[33]. Cardona, M., Optical properties and band structure of $SrTiO_3$ and $BaTiO_3$. *Physical Review*, 1965, **140**(2A), 651.
[34]. Doniach, S. and Sunjic, M., Many-electron singularity in X-ray photoemission and X-ray line spectra from metals. *Journal of Physics*, 1970, **C3**, 285–291.
[35]. Scott, J. F., Device physics of ferroelectric thin-film memories. *Japanese Journal of Applied Physics Part 1—Regular Papers Short Notes and Review Papers 38 (4B)*, 1999, 2272–2274.
[36]. Cardona, M. and Christensen, N. E., Acoustic deformation potentials and heterostructure band offsets in semiconductors. *Physical Review B*, 1987, **35**(12), 6182.
[37]. Ahn, K. H., Baik, S. and Kim, S. S., Significant suppression of leakage current in $(Ba,Sr)TiO_3$ thin films by Ni or Mn doping. *Journal of Applied Physics*, 2002, **92**(5), 2651–2654.
[38]. Hwang, C. S., Lee, B. T., Kang, C. S., Kim, J. W., Lee, K. H., Cho, H. J., Horii, H., Kim, W. D., Lee, S. I., Roh, Y. B. and Lee, M. Y., A comparative study on the electrical conduction mechanisms of $(Ba_{0.5}Sr_{0.5})TiO_3$ thin films on Pt and IrO_2 electrodes. *Journal of Applied Physics*, 1998, **83**(7), 3703–3713.
[39]. Baniecki, J. D., Laibowitz, R. B., Shaw, T. M., Saenger, K. L., Duncombe, P. R., Cabral, C., Kotecki, D. E., Shen, H., Lian, J. and Ma, Q. Y., Effects of annealing conditions on charge loss mechanisms in MOCVD $Ba_{0.7}Sr_{0.3}TiO_3$ thin film capacitors. *Journal of the European Ceramic Society*, 1999, **19**(6–7), 1457–1461.
[40]. Koerber, C., Klein, A., Harvey, S. and Mason, T., Barrier heights at the SnO_2/Pt interface: in-situ photoemission and electrical properties, Surface Science, 2008, **602**, 3246–3252.
[41]. Larsen, P. K., Dormans, G. J. M., Taylor, D. J. and Vanveldhoven, P. J., Ferroelectric properties and fatigue of $PbZr_{0.51}Ti_{0.49}O_3$ thin-films of varying thickness—blocking layer model. *Journal of Applied Physics*, 1994, **76**(4), 2405–2413.